Ninth Canadian Conference on
Earthquake Engineering
Ottawa, Ontario, Canada
26-29 June 2007

SEISMIC BEHAVIOUR OF CONCRETE BEAM-COLUMN JOINTS REINFORCED WITH SUPERELASTIC SHAPE MEMORY ALLOYS

M.S. Alam[1], M.A. Youssef[2] and M. Nehdi[3]

ABSTRACT

Superelastic SMAs are unique alloys that have the ability to undergo large deformations, but can return to their undeformed shape by removal of stresses. In this study, two beam-column joints have been analyzed under reversed cyclic loading using finite element (FE) analysis to investigate the seismic performance of joints reinforced with superelastic shape memory alloys (SMAs) compared to regular steel. Both joints were chosen from an eight storey-RC building located in the high seismic region of western part of Canada. The building was designed and detailed according to the NBCC 2005 and CSA A23.3-04 recommendations. The first specimen was reinforced using steel reinforcing bars. In the second specimen, SMAs were used as reinforcement at the plastic hinge region. The behaviour of the two specimens under reversed cyclic loading, their load-displacement relationship, and energy dissipation ability were compared. The SMA-reinforced specimen ductility and energy dissipation capacity were comparable to the steel reinforced specimen. The results showed that SMA-reinforced specimen was able to recover most of its post-yield deformation requiring minimum amount of repair even after a strong earthquake.

Introduction

Beam-column joints in reinforced concrete (RC) moment resisting frames are considered the weakest link in a structural system (Park and Paulay 1975). Since 1970's design codes started enforcing stricter seismic provisions for detailing of reinforcing bars in beam-column joints. Joints remain extremely vulnerable during earthquakes (Saatcioglu et al. 1999). It has been emphasized that earthquake resistant structures need to be sufficiently ductile so that they can behave elastically under moderate earthquakes. But it is very difficult to build structural elements that can perform elastically under strong ground motion. In conventional seismic design, reinforcing bars are expected to yield in order to dissipate energy. This results in permanent deformation due to plastic properties of post-yield steel reinforcing bars. If superelastic SMAs could be used as reinforcing bars, the performance might change since these are elite materials that can undergo large inelastic deformations and recover their original shape by stress removal. Properties that made SMA an excellent material from an earthquake engineering perspective include: high strength, large energy hysteretic behaviour, full recovery of strains up to 8%, high resistance to corrosion and fatigue (Wilson and Wesolowsky 2005). Ni-Ti alloy has been found to be the most promising SMA for seismic applications. In seismic design if SMA is used as reinforcement in critical structural elements

[1]Ph.D. candidate, Dept. of Civil and Env. Engineering, The University of Western Ontario, London, ON, N6A 5B9,
[2]Asst. Professor, Dept. of Civil and Env. Engineering, The University of Western Ontario, London, ON, N6A 5B9,
[3]Assoc. Professor, Dept. of Civil and Env. Engineering, The University of Western Ontario, London, ON, N6A 5B9.

along with conventional steel, it can yield under strains caused by seismic loads, but potentially recover deformations at the end of earthquake events (Wang 2004).

SMAs have gained increased usage in structural applications. For instance, Dolce et al. (2004) used SMA bracings for seismic retrofitting of existing frames. Maji and Negret (1998) used SMA wires/tendons in prestressed concrete. Indirli et al. (2001) utilized SMA rods for strengthening structures through application of corrective post-tensioning forces. Inaudi and Kelly (1994), Clark et al. (1995) and others contributed significant analytical and experimental studies on structural response control using SMAs. Recent research in the application of SMAs in vibration control includes the work of DesRoches and Delemont (2002), Wilde et al. (2000) and others.

Since SMA is a costly material, it was not until 2004, that it found its way as reinforcing bars in RC structures. To the best of the authors' knowledge, only two research works have been reported, in which SMA rebars have been used as reinforcement in structures subjected to cyclic loading. Wang (2004) used SMA rods in the plastic hinge area of RC columns and evaluated the seismic performance of these columns. Two quarter-scale spiral RC columns with SMA longitudinal reinforcement in the plastic hinge area were designed for laboratory shake table testing. Each specimen was subjected to a series of scaled motion amplitudes. It was observed that the SMA reinforced concrete columns were superior to the conventional steel reinforced concrete columns in limiting relative column top displacement and residual displacements. Also, they withstood larger earthquake amplitudes than the conventional ones. The shake table data showed that SMA RC columns were able to recover nearly all of the post-yield deformation, thus requiring minimal repair. This indicates that there are several opportunities for research work in the application of SMA reinforcements in concrete structures. SMA rebars have a potential to be used in RC beam-column joints in highly seismic zones. Ocel et al. (2004) have used SMAs in steel beam-column connections, which displayed repeatable and stable hysteretic behaviour.

In this paper, superelastic SMAs have been proposed to be used as reinforcements in conjunction with steel in RC beam-column joints. The present study briefly reviews the failure mechanism of RC beam-column joints and addresses a new philosophy for design purposes. Nonlinear finite element (FE) analysis technique has been implemented in this study to demonstrate and compare the performances of SMA-steel-RC beam-column joint and regular steel-RC beam-column joint under reversed cyclic loading. It has been found that SMA-steel-RC beam-column joints are advantageous over steel-RC beam-column joints because of its recentering capability even after large displacements.

Design Philosophy of Beam-Column Joints

A number of researchers e.g. Megget and Park (1971), Meinheit and Jirsa (1981), Meggeta (2003) and others devoted significant effort studying the seismic behaviour of RC joints as well as on the development of design recommendations for ensuring adequate connection behaviour in frame structures. Beam-column joint might fail due to hinging in the column, the beam or the beam-column joint itself. Weak column/strong beam contradicts failure hierarchy of the design capacity concept. Hinging in the joint allows excessive rotations both in the beam and column in conjunction with a loss of load carrying capacity of the column. Weak beam/strong column is the most favourable case since it is not associated with the loss of axial load carrying capacity, i.e. failure in the beam is less critical than that in the column. Current design standards require designing weak beam-strong column philosophy.

RC structures are subjected to severe damage and collapse during strong earthquakes. In the past, conventional structures were mostly designed for safety conditions, where earthquake energies were dissipated through yielding of reinforcement and its inelastic deformation. Structures were allowed to undergo severe damage – this meant saving lives at the expense of structures incurring huge economic losses. More recently the vision has been broadened where the designers no longer want to surrender their own creations/constructions. The seismic design of structures has evolved towards performance-based design in which there is need for new structural members and systems that possess enhanced deformation capacity and ductility, higher damage tolerance, concrete confinement, decreased or

minimized residual crack sizes, recovered and reduced permanent deformations.

The design of ductile moment-resisting frames attempts to force the structure to respond in a strong column-weak beam action in which plastic hinges induced by seismic forces form at the ends of beams. The hinging regions are detailed to allow plastic hinges to undergo yielding in both positive and negative moment, thus ensuring a substantial amount of energy dissipation during earthquakes. If superelastic SMA is used as reinforcements instead of steel in the desired hinge locations of beams, it will not only be able to dissipate higher seismic energy than conventional steel reinforcement, but will also be able to restore its original shape after the seismic event. Because of its higher cost compared to other construction materials, SMA longitudinal rebars will be used along with steel rebars, and SMAs are placed particularly in the hinge regions of beams. If such a RC beam-column joint can be built, this will allow structural engineers to design connections for low/moderate shear distortions and rotations, exhibiting little damage, and eliminating post earthquake joint repairs (Parra-Montesinos et al. 2005).

Finite Element Analysis of Beam-Column Joint

In the present paper, several inelastic time-history analyses have been performed to predict the performances of RC structural elements using a FE program. Fibre modelling approach has been employed to clearly represent the distribution of material nonlinearity along the length and cross-sectional area of the member. 3D beam-column elements have been used for modelling the beam and column where the sectional stress-strain state of the elements is obtained through the integration of the nonlinear uniaxial stress-strain response of the individual fibres in which the section has been subdivided, completely following the spread of material inelasticity within the member cross-section and along the member length. Concrete and steel has been modelled using models of Martinez-Rueda and Elnashai (1997) and Monti and Nuti (1992), respectively. SMA has been modelled according to the model of Auricchio and Sacco (1997). Figure 1 shows the 1D-superelastic model used in the FE program where SMA has been subjected to multiple stress cycles at a constant temperature and undergoes stress induced transformation. The parameters used to define the material model are: 1) yield stress, f_y; 2) maximum stress up to superelastic strain range, f_{P1}; 3) first stage of unloading stress, f_{T1}; 4) second stage of unloading stress, f_{T2}; 5) superelastic plateau strain length, ε_l and 6) modulus of elasticity, E.

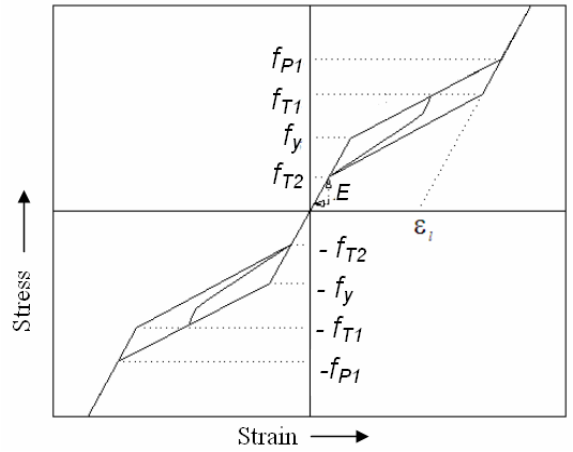

Figure 1. 1-D-Superelastic model of SMA (Auricchio and Sacco 1997) incorporated in the FE program.

Validation of the Program

This section describes two analyses that were used to validate the results of the FE program.

Case 1: Steel-RC Joint

Said and Nehdi (2004a) tested a full-scale RC beam-column joint designed as per the CSA A23.3-94 (1994) requirements under reversed cyclic load. A FE mesh has been developed for the beam-column joint where the geometry and material properties were taken from the experimental data provided by Said and Nehdi (2004a). Figure 2a presents the experimental results of the tested specimen showing the beam tip load versus beam tip displacement up to its ultimate load. Figure 2b illustrates the numerical results predicted by the FE analysis. The ultimate beam tip load was predicted as 127 kN at a tip displacement of 141 mm compared to the experimental results where the tip load was 138 kN at a tip displacement of 143 mm. The total predicted energy dissipation was 131 kN.m, which is 13% smaller than the experimental value. The numerical results show that the FE program is capable of predicting the behaviour of the joint with reasonable accuracy.

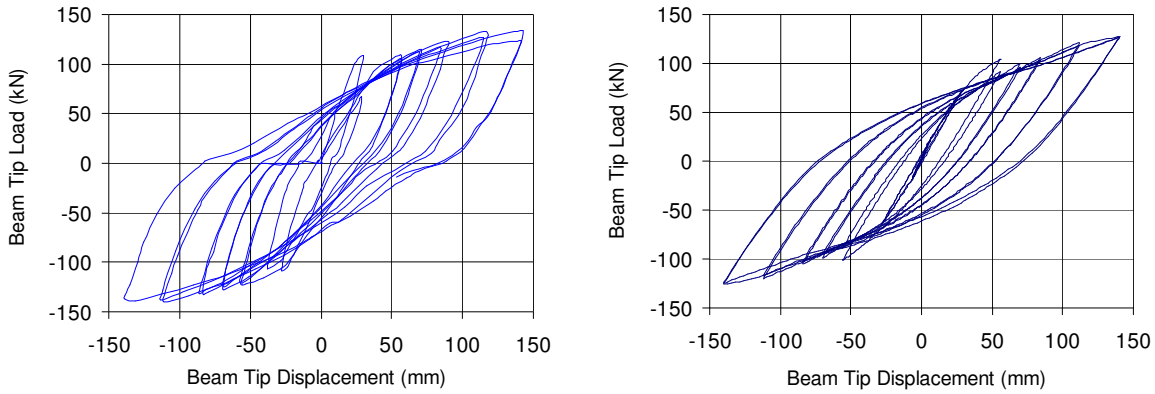

(a) Experimental Results (Said and Nehdi 2004a) (b) Numerical Results

Figure 2. Beam tip-load versus tip-displacement for steel-RC beam column.

Case 2: SMA-Steel-RC Joint

Two quarter-scale spiral RC columns representing RC bridge piers were designed, constructed and tested using a shake table by Wang (2004). The bridge pier was reinforced with SMA rebars placed at the plastic hinge region and connected to the steel rebars with mechanical couplers. Figure 3a shows the experimental results of the bridge pier with excellent recentering capability when subjected to base acceleration.

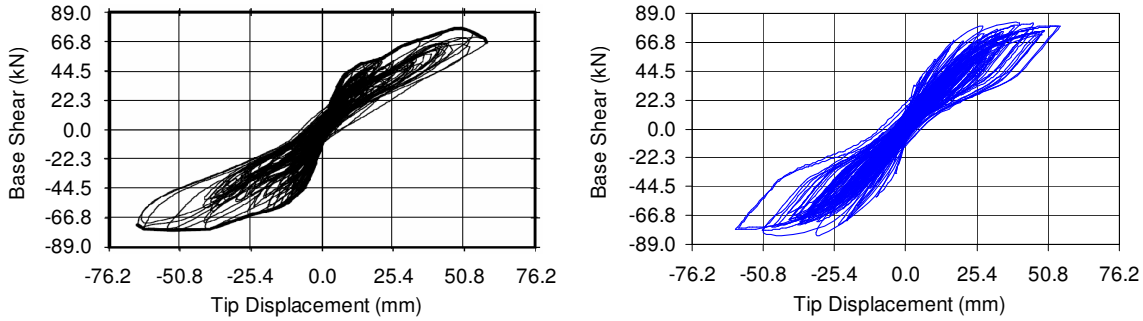

(a) Experimental results (Wang 2004) (b) Numerical results

Figure 3. Base shear versus tip-displacement for SMA-steel-RC bridge pier.

FE analysis has been performed to predict the performance of the bridge pier tested by Wang (2004). SMA has been modeled according to Fig. 1. Figure 3b depicts the predicted base shear-tip displacement

of the numerical model which seems to be fairly accurate as compared to the experimental results of Wang (2004) shown in Fig. 3a. The maximum base shear and the tip displacement were predicted as 81.5 kN and 62.0 mm compared to experimental values of 77.2 kN and 66.0 mm, respectively. The numerical results show good agreement with the experimental results which varies by only 5.6% for base shear and 6.1% for tip displacement. The accumulated energy dissipation was predicted as 48,160 kN.mm from the predicted load-displacement curve where as the experimental value was 44,010 kN.mm (9.4% lower than the predicted value). The displacement ductility was measured as 5.9 compared to 6.7 predicted analytically.

Case Study

It has been observed that medium rise buildings are more susceptible to damage during an earthquake (Bariola 1992). An eight-storey RC moment resisting frame has been selected in this study. The building has been designed and detailed in accordance with Canadian Standards (CSA A23.3-04) assuming that it is located in the western part of Canada on firm ground with un-drained shear strength of more than 100 kPa. The elevation and plan of the building is shown in Fig. 4. The design PGA is 0.54g and the moment frames are designed with moderate level of ductility. An exterior beam-column joint has been isolated at the points of contraflexure from the mid-height of fifth floor to the mid-height of sixth floor (Joint A in Fig. 4a). It is to be noted that this study is a part of an experimental project. The present study is conducted to predict the experimental results prior to testing. The size of the test specimens has been reduced by a factor of ¾ to accommodate the laboratory space and equipment limits. The forces acting on the joints were also scaled down by a factor of $(¾)^2$. This factor has been chosen to maintain the stresses in the scaled models similar to the full-scale joint.

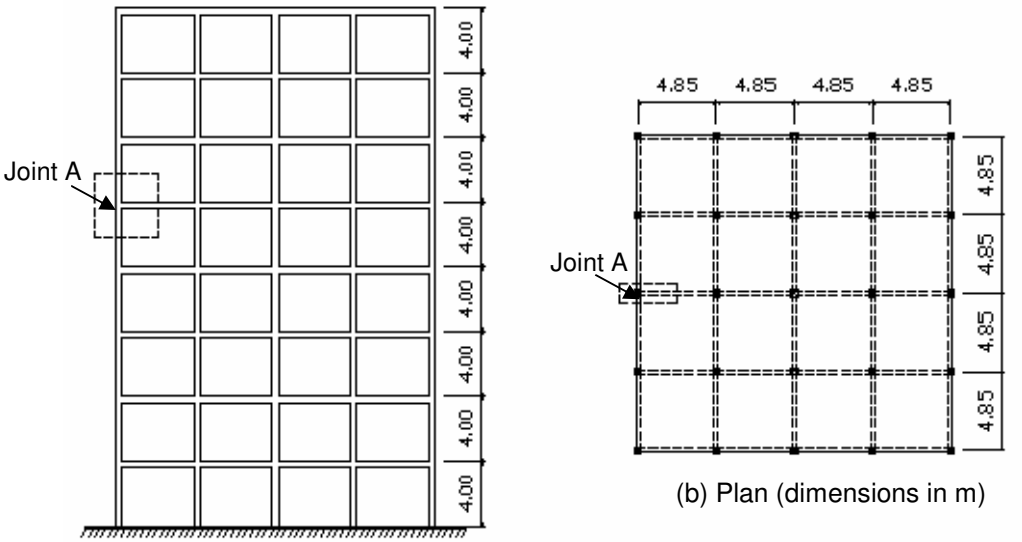

Figure 4. 8-storey frame building located in the western part of Canada.

Two beam-column joint specimens will be considered in this study. One will be reinforced with regular steel bars (specimen JBC-1), while the other will be reinforced with SMA at the plastic hinge region of the beam and regular steel in the remaining portion of the joint (specimen JBC-2). The detailed design of joints JBC-1 and JBC-2 are given in Fig. 5. The assumed material properties are presented in Table 1. The beam and the column have been designed with the maximum moment and shear forces developed during the analysis of the building considering all possible combinations of load cases. The column axial force, P has been taken from the analysis of the corresponding load case for which the column has been designed and is found originally as 460.0 kN, after scaling down P becomes 258.8 kN. The reduced cross section of the column is chosen as 250 x 400 mm with 4-M20 longitudinal rebars corresponding to a 1.2% reinforcement ratio (M20 is equivalent to 19.5 mm diameter bar). The column is transversely reinforced with M10 closed rectangular ties spaced at 80 mm in the joint region (±640 mm from the face of the joint)

and then spaced at 115 mm elsewhere. The top and bottom longitudinal reinforcements of the beam of specimens JBC-1 and JBC-2 are 2-M20 bars and 2-SMA20 bars (SMA20 is equivalent to 20.6 mm diameter bar) corresponding to 1.2% and 1.5% reinforcement ratio, respectively. For both specimens the ties were spaced at 80 mm for 800 mm of the beam adjacent to the column and then spaced at 120 mm. The size of longitudinal rebar and the size and spacing of the transverse reinforcement for the joint conform to the current code requirements (CSA A23.3-04).

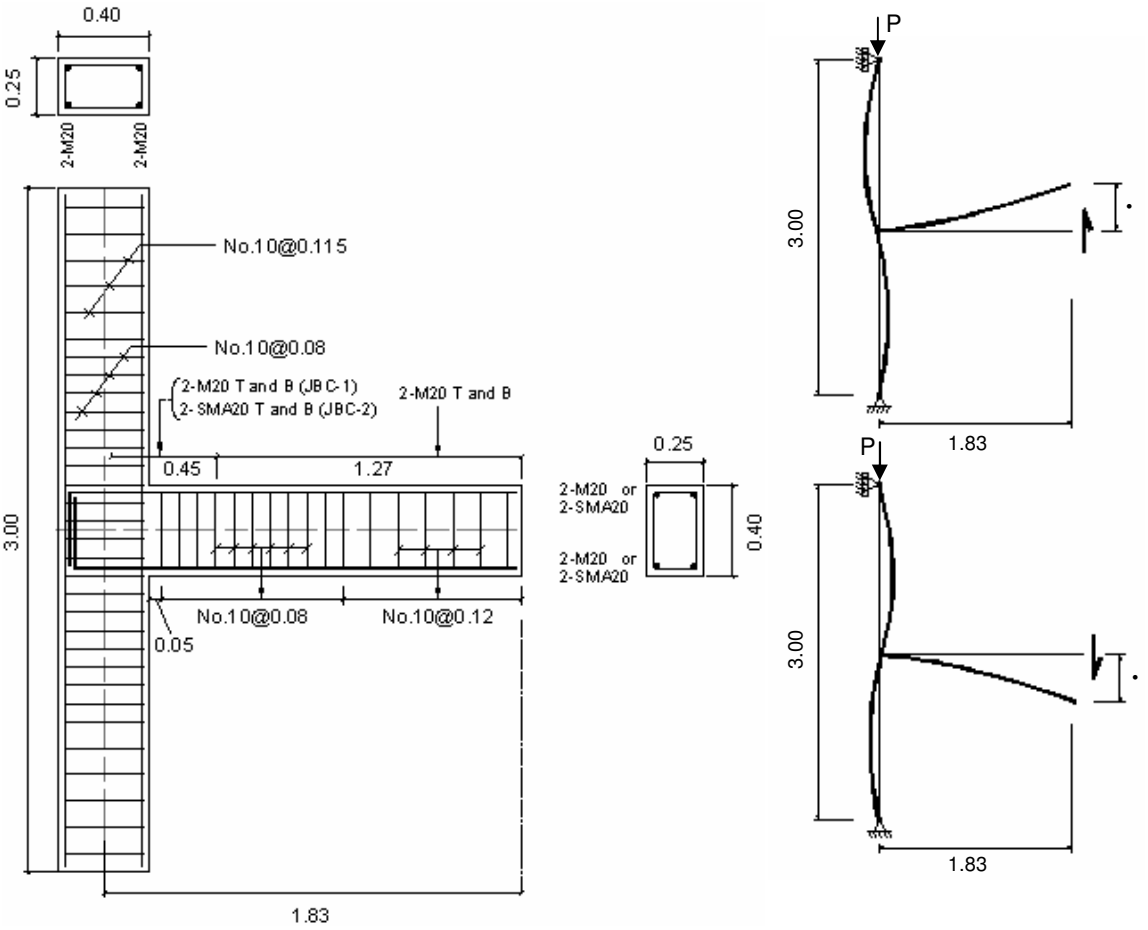

(a) (b)

Figure 5. (a) Reinforcement details of specimen JBC-1 and JBC-2, (b) typical deflected shape of the specimens under reversed cycle of tip-displacement (dimensions in m).

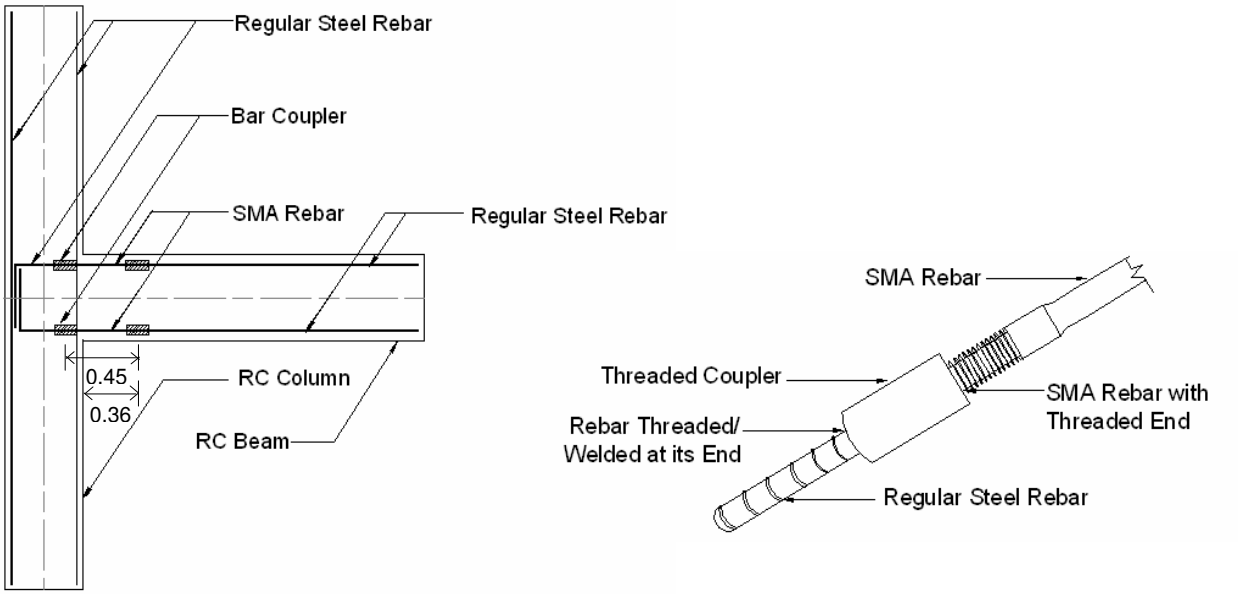

(a) (b)

Figure 6. (a) Splice details of specimen JBC-2, (b) threaded mechanical coupler connecting SMA rebar with regular steel rebar (all dimensions in m).

The geometry, longitudinal and transverse reinforcement arrangements of the columns are the same for both the specimens. In beam, JBC-1 and JBC-2 are similar in terms of geometry, and transverse reinforcement and its arrangement. JBC-2 is having SMA as longitudinal reinforcement instead of regular steel in JBC-1 at its plastic hinge. The plastic hinge length is calculated as 360 mm (Paulay and Priestley 1992) for JBC-2 from the face of the column. Mechanical couplers have been used to connect SMA with regular steel rebar. The total length of SMA is 450 mm from the centre to centre of the coupler as shown in Fig. 6. Figure 5b shows the idealized support conditions and typical deflected shape of the joint under reversed cycles of tip-displacement.

Table 1. Material properties used in the FE program.

Material	Property	Value
Concrete	Compressive strength (MPa)	50.9
	Strain at peak stress (%)	0.18
	Modulus of Rupture (MPa)	4800
M20 Steel	Yield Strength (MPa)	500
	Strain hardening parameter (Post yield stiffness/initial stiffness)	0.03
M10 Steel	Yield Strength (MPa)	450
SMA20	Modulus of elasticity, E_{SMA} (MPa)	64000
	f_y as in Fig. 1 (MPa)	400
	f_{P1} as in Fig. 1 (MPa)	510
	f_{T1} as in Fig. 1 (MPa)	370
	f_{T2} as in Fig. 1 (MPa)	225
	ε_l as in Fig. 1 (%)	6.00

Results and Discussions

The two exterior beam-column subassemblages JBC-1 and JBC-2 are analyzed under reversed cyclic displacements. Displacement controlled loading cycle is applied at the beam-tip. Figure 7a and 7b show the load-deflection curves for specimen JBC-1 and JBC-2, respectively. In case of JBC-1, the first flexural crack was observed at a load of 20.5 kN. The top steel yielded at a load of 56.6 kN and the bottom steel yielded at 57.1 kN load. The maximum load was found as 58.1 kN. Figure 8a and 9a show the strain measurements close to the column face in the beam main top and bottom steel reinforcing bars respectively. It can be observed from the force-displacement relationship of JBC-1 (Fig. 7a) that when the force drops to zero there was large residual displacement at the beam-tip (84 mm) with significant amount of strain at beam rebars at the column face (Fig. 8a and 9a). In case of JBC-2, the first flexural crack was observed at a load of 19.3 kN. The top SMA yielded at a load of 51.6 kN and the bottom SMA yielded at a load of 53.7 kN. However, the maximum load was found to be 71.8 kN in the whole loading cycle. In the second specimen, the exterior concrete of the beam close to the column face reached its peak stress at a load of 64.0 kN. As the load continued, the joint started to produce larger loads with the core concrete still within the peak strain. Figure 8b and 9b show the strain measurements close to the column face in the beam main top and bottom SMA reinforcing bars respectively. Both the diagrams show flag shaped response under tension and almost linear response under compression since concrete contributed substantial portion under compression and thus, reducing the demand on SMA rebars. The force-displacement relationship of JBC-2 shows that there will be a very small amount of residual displacement (13.8 mm) at the beam tip at zero force which is due to almost zero strain in SMA rebar (Fig. 8b and 9b).

Comparison between JBC-1 and JBC-2

SMA and steel have different properties. The modulus of elasticity of SMA is 1/3 of steel modulus. The yield strength of SMA and steel were 400 and 500 MPa, respectively. The diameter of SMA rebar was 20.6 mm compared to that of steel diameter 19.5 mm. The concrete compressive strength was the same for both the specimens. The presence of couplers in JBC-2 reduced the effective depth by 10 mm compared to JBC-1. This led to the development of an early crack in JBC-2. The concrete clear cover was considered as 17 mm for both specimens.

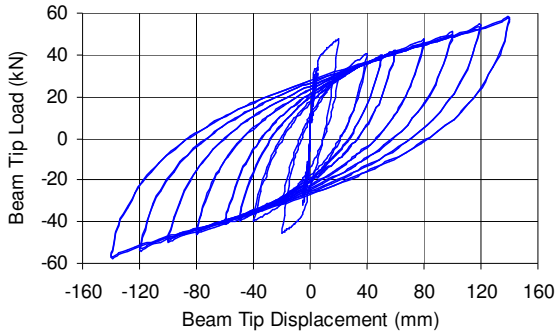

(a) Steel-RC beam-column joint (JBC-1)

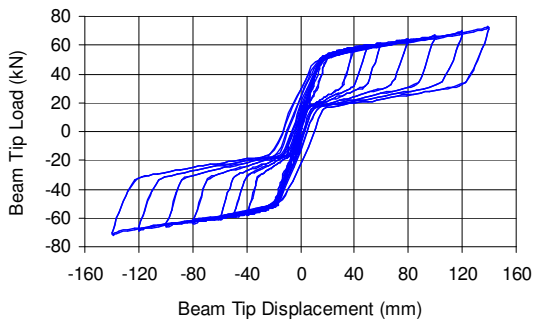

(b) SMA-steel-RC beam-column joint (JBC-2)

Figure 7. Beam tip load-displacement relationship.

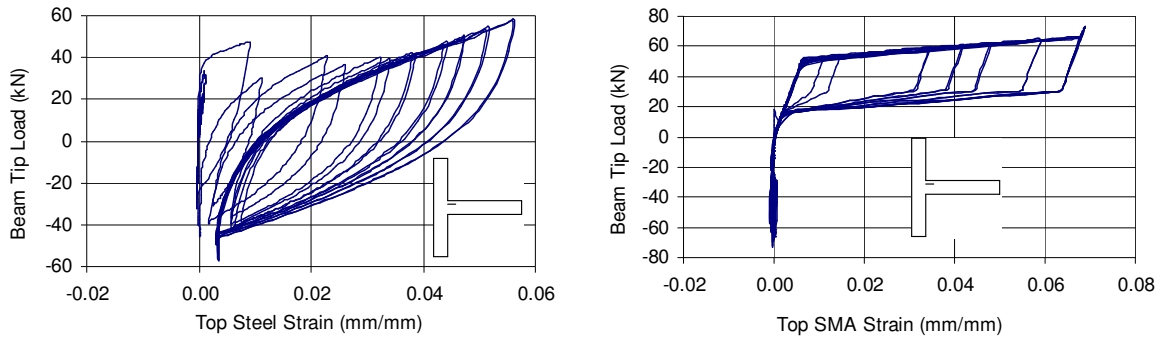

(a) Steel-RC beam-column joint (JBC-1) (b) SMA-steel-RC beam-column joint (JBC-2)

Figure 8. Beam tip load versus strains in beam main top bar at face of column.

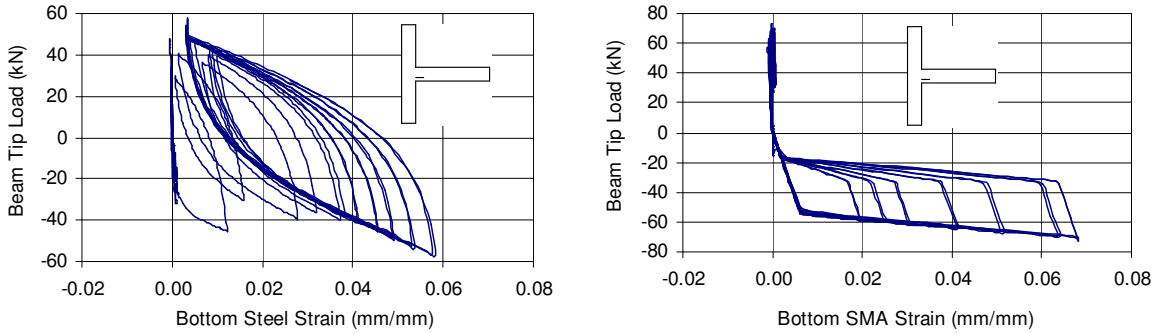

(a) Steel-RC beam-column joint (JBC-1) (b) SMA-steel-RC beam-column joint (JBC-2)

Figure 9. Beam tip load versus strains in beam main bottom bar at face of column.

The superelastic behaviour of SMA rebars resulted in very small residual strain at the joint, whereas the steel rebar is not effective in post-yield strain recovery. This can be clearly observed in the load-displacement hysteretic curves of Figs. 7a and 7b where JBC-1 has large permanent displacements and JBC-2 has very low residual displacement. The amount of energy absorbed by JBC-1 was found as 89882 kN.m whereas by JBC-2 was 69162 kN.m. The results show that JBC-2 dissipated 23% less energy compared to JBC-1 and conventional steel-RC beam-column joint showed better performance in energy dissipation capacity because of its large hysteretic loop. But the advantage of SMA-steel-RC beam-column joint lies in its recentering capability even after large displacements. Thus this kind of joints will be able to dissipate significant amount of energy during an earthquake by undergoing large displacements but potentially recover all of its deformation after the earthquake requiring minimum amount of repairing.

Conclusions

This paper discusses a novel approach to reduce the seismic vulnerability of RC structures by utilizing smart materials like SMA in beam-column joints. The objective of this study is to investigate the cyclic performance of an exterior beam-column joint which has been isolated from an eight-storey building located in high seismic zone of western part of Canada. This joint specimen has been designed according to CSA standards (A 23.3-04) in two ways: one with regular steel rebar (Specimen JBC-1) and the other with superelastic SMA rebar (Specimen JBC-2) at its plastic hinge region. Both specimens JBC-1 and JBC-2 have been analyzed under cyclic displacement loading with the use of a finite element program and their performances have been compared. Before analyzing the beam-column joints, the FE program has been validated using experimental results for beam-column joint reinforced with regular steel and a column-foundation joint reinforced with SMA-steel coupled reinforcement at its plastic hinge location. Both the numerical results indicate that the FE program can predict the hysteretic load-displacement curve with reasonable accuracy.

The analytical results of the hysteretic load-displacement curves of JBC-2 exhibited better performance compared to that of JBC-1 in terms of residual displacements remaining in the joint after unloading. The flag-shaped stress-strain hysteresis of superelastic SMA bars produced flag-shaped hysteretic load-displacement curves in the SMA-steel-RC beam-column joint (JBC-2). Although steel-RC beam-column joint (JBC-1) dissipated relatively higher amount of energy compared to that of JBC-2 because of its large hysteretic loops, still JBC-2 performed better because of its capability in recovering post-elastic strain, which makes it very attractive in high seismic regions where the beam-column joints will be able to dissipate significant amount of energy and remain functional even after a strong earthquake.

Excessive lateral displacements and residual displacements have been identified as the major causes of failure of buildings and bridges during earthquakes. SMAs are unique materials that can recover almost fully even after large inelastic deformations. If SMA can be used as reinforcement in beam-column joints, it can initiate major progress in seismic design whereby the repair cost may be substantially reduced and the structure may remain serviceable even after a severe earthquake.

References

Auricchio, F. and Sacco, E., 1997. Superelastic shape-memory-alloy beam model, *Journal of Intelligent Material Systems and Structures*, 8(6), 489-501.

Bariola, J., 1992. Drift response of medium-rise reinforced concrete buildings during earthquakes, *ACI Structural Journal*, 89(4), 384-390.

Clark, P. W., Aiken, I. D., Kelly, J. M. Higashino, M. and Krumme, R., 1995. Experimental and Analytical Studies of Shape-Memory Alloy Dampers for Structural Control, Proc. SPIE, 2445, 241-251.

Design of Concrete Structures, CSA A23.3-04, Canadian Standards Association, Rexdale, Ontario, Canada, 2004, 240p.

DesRoches, R., McCormick, J. and Delemont, M., 2004. Cyclic Properties of Superelastic Shape Memory Alloy Wires and Bars, *Journal of Structural Engineering, ASCE*, 130(1,) 38-46.

DesRoches, R., and Delemont, M., 2002. Seismic Retrofit of Simply Supported Bridges Using Shape Memory Alloys, *Engineering Structures*, 24(3), 325-332.

Dolce, M., Cardone, D., Marnetto, R., Mucciarelli, M., Nigro, D., Ponzo, F.C. and Santarsiero, G., 2004. Experimental Static and Dynamic Response of a Real RC Frame Upgraded with SMA Re-Centering and Dissipating Braces, Proc. of the *13th World Conf. on Earthquake Engg.*, Canada, Paper no. 2878.

Dolce, M. and Cardone, D., 2001. Mechanical behaviour of shape memory alloys for seismic applications 1: Martensite and austenite NiTi bars subjected to torsion, *International Journal of Mechanical Sciences*, 43, 2631-2656.

Hanson, N. W., and Connor, H. W., 1967. Seismic Resistance of Reinforced Concrete Beam-Column Joints, *Journal of the Structural Division, ASCE Proceedings 5537*, 93(ST5), 533-560.

Inaudi, J. A., and Kelly, J. M., 1994. Experiments on Tuned Mass Dampers Using Viscoelastic, Frictional and Shape Memory Alloy Materials, Proc. First World Conf. on Structural Control, 2(TP3), 127-136.

Indirli, M., Castellano, M.G., Clemente, P., and Martelli, A., 2001. Demo-application of shape memory alloy devices: The rehabilitation of the S. Giorgio Church Bell-Tower," *Proc. of SPIE*, 4330, 262-272.

Maji, A.K., and Negret, I, 1998. Smart Prestressing with Shape Memory Alloy, *Journal of Engineering Mechanics*, 124(10), 1121-1128.

Martinez-Rueda, J.E., and Elnashai, A.S., 1997. 1997. Confined concrete model under cyclic load, *Materials and Structures*, 30(3), 1997, pp. 139-147.

Megget, L. M., and Park, R., 1971. Reinforced Concrete Exterior Beam-Column Joints under Seismic Loading, *New Zealand Engineering (Wellington)*, 26(11), 341-353.

Meggeta, L.M., 2003. The Seismic Design and Performance of Reinforced Concrete Beam-Column Knee Joints in Buildings, *Earthquake Spectra*, 19(4), 863-895.

Meinheit, D. F., and Jirsa, J. O., 1981. Shear Strength of RC Beam-Column Connections, *Journal of Structural Division, ASCE*, 107(ST. 11), 2227-2244.

Miyazaki, S., Imai, T., Igo, Y., and Otsuka, K., 1986. Effect of cyclic deformation on the pseudoelasticity characteristics of Ti–Ni alloys, *Metall. Trans. A,* 17A, 115–120.

Monti, G., and Nuti, C., 1992. Nonlinear cyclic behaviour of reinforcing bars including buckling, *Journal of Structural Engineering*, 118(12), 3268-3284.

Mugurama, H., Nishyiyama, M. and Watanabe, F., 1995. Lessons Learned from Kobe Earthquake – A Japanese Perspective, *PCI Journal*, a Special Report, 28-42.

National Building Code of Canada, 2005, National Research Council, Canada.

Ocel, J., DesRoches, R., Leon, R. T., Hess, W. G., Krumme, R. Hayes, J. R. and Sweeney, S., Steel Beam-Column Connections Using Shape Memory Alloys, *Journal of Structural Engineering, ASCE*, 130(5), 732-740.

Orgeas, L., Liu, Y. and Favier, D., 1997. Experimental study of mechanical hysteresis of NiTi during ferroelastic and superelastic deformation, *Journal De Physique. IV : JP*, 7(5), C5-477-C5-482.

Park, R. and Paulay, T., 1975. Reinforced Concrete Structures, *John Wiley & Sons Inc*, New York, 769 p.

Parra-Montesinos, G.J., Peterfreund, S.W., and Chao, S., 2005. Highly Damage-Tolerant Beam-Column Joints Through Use of High-Performance Fiber-Reinforced Cement Composites, ACI Structural Journal, 102(3),487-495.

Saatcioglu, M., Mitchell, D., Tinawi, R., Gardner, N.J., Gillies, A.G., Ghobarah A., and Anderson, D.L., Lau, D., 2001. The August 17, 1999, Kocaeli (Turkey) Earthquake - Damage to Structures, *Canadian Journal of Civil Engineering*, 28(4), 715-737.

Said, A.M., and Nehdi, M.L., 2004. Use of FRP for RC Frames in Seismic Zones: Part I. Evaluation of FRP Beam-Column Joint Rehabilitation Techniques, *Applied Composite Materials*, 11(4), 205-226.

Wang, H., 2004. A Study of RC Columns with Shape Memory Alloy and Engineered Cementitious Composites, *M. Sc. Thesis*, Department of Civil Engineering, University of Nevada, Reno, 297 p.

Wilde, K., Gardoni, P. and Fujino, Y., 2000. Base Isolation System with Shape Memory Alloy Device for Elevated Highway Bridges, *Engineering Courses*, 22, 222-229.

Wilson, J.C., and Wesolowsky, M.J., 2005. Shape Memory Alloys for Seismic Response Modification: A State-of-the-Art Review, *Earthquake Spectra*, 21(2), 569-601.